NUMERICAL VALIDATION ON THE PERFORMANCE OF A TWO DIMENSIONAL CURVED DIFFUSER

Khalaf I. Hamada

Assistance Lecturer

Mech. Eng. Dept. –University of Tikrit

ABSTRACT

This paper deals with the investigation of the characteristic of subsonic viscous flow through a curved diffuser numerically with commercial code for computational fluid dynamics (CFD) Fluent Inc. version 6.3. The diffuser flow is a two-dimensional, turbulent, incompressible and fully developed. The investigations are based on the Spalart-Allmaras turbulent model. A 2-D quadrilateral grid is generated by the grid generator GAMBIT. Obtained results are compared with the available experimental data and found to give good agreement. The effects of curvature angle, area ratio and adding tail channel with constant area on the diffuser performance and flow pattern are studied and revealed by the pressure contour, velocity vector, and variation of the pressure recovery factor for all above mentioned parameters.

Key words: **Diffuser performance, CFD, Turbulent flow**

Nomenclatures:

AR	**Area ratio(exit area/inlet area)**	x,y	Coordinate system(m)
AS	Aspect ratio(channel width/channel height)	**Greek symbols**	
C_p	Pressure recovery factor	α	Divergence angle(deg.)
D	Hydraulic diameter at entrance(m)	ë	Gradient
L	Length of tail channel(m)	θ	Curvature angle(deg.)
P	Pressure(N/m^2)		Kinematic viscosity(m^2/s)
Re	**Reynolds number**	ρ	Density(kg/m^3)
t	Time(sec.)	**subscript**	
U	Velocity(m/s)	i,j	Coordinate index
u,v	Velocity components(m/s)	t	Turbulent

INTRODUCTION

Diffusers represent integral parts of jet engines and many other applications that depend on fluid flow. Performances of a propulsion system and ducts for the air conditioning systems as a whole are dependent on the efficiency of diffusers. These devices concern with converting velocity head to static pressure and for reducing velocities. Identification of separation within diffusers is important since separation increases drag and causes inflow distortion to engine fans and compressors[1]. Well designed diffusers should incur minimal total pressure losses and deliver nearly uniform flow with small transverse velocity components at the engine compressor entrance[2]. Reduced total pressure recovery lowers propulsion efficiency, where as non uniform flow conditions at the engine face lower engine surge and stall limits. However, airframe weight and space considerations demand as short as possible diffuser, resulting in high degrees of centerline curvature and large changes in cross sectional area. These factors are responsible for the development of strong secondary flow and attendant boundary layer separation,

which increase total pressure non uniformity and total pressure loss at the diffuser exit. Large amounts of distortion significantly reduce engine performance and may lead to drastic results, such as engine stall[2].

The flow field characteristics and performance of subsonic diffusers has been an interesting research topic for many years. Sprenger[3] presented experimental study to investigate efficiency for a straight-conical diffuser and two circular curved diffusers. The first one with angle of curvature ($=15^{\circ}$) and the second with ($=30^{\circ}$). All diffusers with angle of divergence ($=8^{\circ}$) and area ratio (AR=4). The results show that efficiency (the ratio of actual static pressure rise to that ideally obtained by neglecting any pressure loss when ever in the diffuser) decrease as the angle of curvature increased. Majumdar and Agrawal[4] performed an experimental study for air flow in a curvature diffuser with (AR=3.4),($=90^{\circ}$) and (AS=0.685) after inserting a row of vans at the diffuser inlet to control the changing of entrance angle of air to the diffuser. Results showed that when air enter to the diffuser with an angle of 100 $^{\circ}$ toward

convex wall led to a big development of flow distribution inside diffuser from separation occurrence on the convex wall diffuser, as well as increasing in pressure recovery factor. Singh et. al[5] performed experimental study for turbulent air flow with growth of thin boundary layer through curved diffuser with (=90º), (AR=2) and (AS=6) with additional constant cross sectional area duct at the diffuser exit and (Re=2.2*105) at inlet. Results show that the pressure recovery factor and losses factor in total pressure were (51%, 15%) respectively. Numerical investigation for turbulent flow through a curved squared duct(=1800 º) carried out by Y.D. Choi et. al.[6]. They constructed some of numerical modeling and select the best one to represent the inner wall for the curved U-duct by very small meshing to cover boundary sub-layer by using parabolic sub-layer approximation (PSL) method. This approach ignore static pressure variation inside this sub-layer, and using the algebraic second-moment (AMS) and compression with [(k-) Eddy-viscosity model], and they found good agreement with experimental results which presented by S. Chang et. al.[7].

The present work aims to numerically solve the flow through a curved diffuser and compare the predicted results with Al-Annaz's work[8] computationally, focusing on three aspects of CFD modeling and their effects on the diffuser flow computations. The first part focuses on the effect of curvature angle on the flow pattern and diffuser performance. Secondly, the effect of area ratio on the flow pattern and diffuser performance has to be carried out. Finally, the effect of adding a tail channel on the flow pattern and diffuser performance is to be focused. This study has been done employing a computational-fluid dynamics (CFD) code not only to obtain aerodynamic parameter C_p, but also to study the physics of flow.

COMPUTATIONAL ETHODOLOGY

Diffuser flow computations are particularly a challenging task for Computational Fluid Dynamics (CFD) simulations due to adverse pressure gradients created by the decelerating flow, frequently resulting in separation[1]. These separations are highly dependent on local turbulence level, viscous wall effects, and diffuser pressure ratio, which

are functions of the velocity gradient and the physical geometry. Thus, turbulence modeling and geometry modeling become dominant factors that affect the ability of CFD to accurately predict flow through diffusers.

1-Governing Equations and Turbulence Model Selection:

The mean flow satisfies the incompressible Navier-Stokes equations with an eddy viscosity:

$$\ddot{e}U \ N \ 0 \qquad \ldots\ldots\ldots\ldots \quad (1)$$

$$U.\ddot{e}U \ N \ > \ddot{e}P < \ddot{e}.|\theta\hat{} < \hat{}_t\ \ddot{e}U\|\ \ldots. \ (2)$$

Turbulence modeling is a major stage in computational fluid dynamics. It is unfortunate fact that no single turbulence model is universally accepted as being superior for all classes of problems. The choice of turbulence model should depend on several considerations such as the physics encompassing the flow, the established practice for a specific class of problems. Furthermore, the level of accuracy required and the available computational resources and the time available for the simulation. To make the

most appropriate choice of model for any application, one must understand the capabilities and limitations of various options.

In the present work, the Spalart & Allmaras turbulence model was considered to determine the turbulent viscosity. The Spalart-Allmaras model was designed specifically for aerospace applications involving wall-bounded flows and has been shown to give good results for boundary layers subjected to adverse pressure gradients. It is also gaining popularity for turbomachinery applications[9].

This model belongs to only one equation family of eddy viscosity models. This family is based on the assumption that Reynolds stress-tensor $> ....\overline{\mathbf{u}\frac{1}{4}\mathbf{v}\frac{1}{4}}$ is related to the mean strain rate through an apparent turbulent viscosity called eddy viscosity υ_t, which can be computed from Reynolds stresses[9]:

$$> \overline{\mathbf{u' v'}} \ N \ \hat{}_{\mathbf{t}} \ \frac{Ð\overline{\mathbf{u}}}{Ð\mathbf{y}} < \frac{Ð\overline{\mathbf{v}}}{Ð\mathbf{x}} \qquad \ldots\ldots\ldots \ (3)$$

Actually, the computation uses an intermediate transport variable **˜** with the damping function $\mathbf{f}\hat{}_{\mathbf{1}}(\mathsf{t})$ relating to

turbulent viscosity by $\hat{}_t N \tilde{}.f_{\hat{}1}(t)$ to solve the following transport equation[9]:

$$\frac{Ð\tilde{}}{Ðt} < \frac{Ð}{Ðx_i} \vartheta\tilde{}u_i : N\, G_{\hat{}}$$

$$< \frac{1}{\dagger\sim} \frac{Ð}{Ðx_j} \left[\vartheta_{\hat{}} < \tilde{}. \frac{Ð\tilde{}}{Ðx_j} \right] < C_{b2}. \left[\frac{Ð\tilde{}}{Ðx_j} \right]^2$$

$$> Y_{\hat{}}$$

………………... (4)

The intermediate variable $\tilde{}$ is in general identical to the turbulent kinematic viscosity υ_t except in the near-wall (viscous-affected) region. G_υ and Y_υ are the production and destruction terms of turbulent viscosity respectively. Both are strong in the near-wall region due to wall blocking and viscous damping. Besides $\dagger\sim$ denotes the turbulent Prandtl number, C_{b2} a calibration constant and $_{\hat{}}$ is the molecular kinematic viscosity. The first term will be vanished due to steady flow assumption for the present study.

Turbulent Viscosity Modeling[9]:

The turbulent kinematic viscosity, $_t$, is computed from:

$$\hat{}_t N \tilde{}.f_{\hat{}1} \qquad ……………………(5)$$

Where the viscous damping function, f 1, is given by:

$$f_{\hat{}1} N \frac{t^3}{t^3 < C_{\hat{}1}} \quad \text{with } t\, \hat{O}\, \frac{\tilde{}}{\hat{}} \quad ….. (6)$$

Turbulent Production Modeling[9]

The production term, G , is modeled as

$$G_{\hat{}} N C_{b1}\tilde{S}\tilde{} \qquad ……… (7)$$

where

$$\tilde{S} = S + \frac{\tilde{}}{|^2 d^2} f_{\hat{}2}$$

and $\quad f_{\hat{}2} N 1 > \dfrac{t}{1 < t f_{\hat{}1}}$

Cb1 and are constants, d is the distance from the wall, and S is a scalar measure of the deformation tensor. By default in FLUENT, as in the original model proposed by Spalart and Allmaras, S is based on the magnitude of the vorticity:

$$S N \sqrt{2 h_{ij} h_{ij}} \qquad …..................(8)$$

Where ij is the mean rate-of-rotation tensor and is defined by

$$h_{ij} \; N \; \frac{1}{2} \left(\frac{\partial u_i}{\partial x_j} > \frac{\partial u_j}{\partial x_i} \right) \qquad \dots\dots (9)$$

Turbulent Destruction Modeling[9]

The destruction term is modeled as

$$Y \sim \; N \; C_{w1} f_w \left(\frac{\tilde{}}{d} \right)^2 \qquad \dots\dots\dots (10)$$

where

$$f_w = g \left[\frac{1 + C_{w3}^6}{g^6 + C_{w3}^6} \right]^{1/6} ,$$

$$g \; N \; r < C_{w2} \left(r^6 > r \right) \; \text{and} \; r \; Ô \; \frac{\tilde{}}{\tilde{S}|^2 d^2}$$

Cw1, Cw2, and Cw3 are constants. Note that the modification described above to include the effects of mean strain on S will also affect the value of $\tilde{S}$ used to compute r. The model constants Cb1; Cb2; $^\dagger \tilde{}$; C 1; Cw1; Cw2; Cw3 and have the default values[10] in Table(1).

2-Numerical Tools and Models

The FLUEN6.3 CFD code[9], uses a cell-centered finite volume method. The flow field itself is solved using Navier-Stokes Equations with an eddy viscosity and additional one-equation turbulence model [Spalart-Allmaras model]. For the present study, the solver was configured to run with perfect gas, (air =1.4, the same properties of air in the ref.[8]), 2-D, steady state, incompressible and subsonic flow. The implicit method implemented uses a pressure based solution method. Note, all internal number representation in the solver utilized double precision and the schemes used here are second order. The SIMPLE algorithm with under relaxation coefficients is used in the overall discretization of the equations, while the under relaxation factors which used are taken as follows: for pressure (0.3), for density (0.9), for body force (0.85), and for momentum (0.7). To reduce the dispersion errors and to increase the speed of the computations, the multigrid approach has also been used.

3-Computations

The computational domain models the experimental apparatus of Al-Annaz[8] (see fig.(1)). In the 2-D simulation for curved diffuser with details in Table (2) are undertaken.

The computational domain for this study is bounded by two curved wall surface, one inlet and one outlet conditions as

shown in Fig(2). The boundary conditions used for the curved diffuser are velocity inlet, outflow and wall surface. The inlet uses specified velocity profile, while the outlet is outflow boundary condition. The diffuser walls are modeled to be stationary wall with no-slip boundary condition.

Fluent gives a great importance to properly resolve boundary layers close to surfaces in turbulent flow. Failing to do so will result in erroneous results when calculating bulk values like factor of pressure recovery due to area enlargement. It is much easier to accomplish accurate boundary layers using a structured grid (Note that the solver still treats the grid as an unstructured grid mathematically)[9]. All grids used in this study are therefore structured. Due to the strong interaction of the mean flow and turbulence, the numerical results tend to be more susceptible to grid dependency than those for laminar flows[9]. It is therefore recommended to resolve the near wall regions with sufficiently fine meshes because the mean flow changes rapidly as shown in Fig.(3). The structured grid for this study has been generated using the grid generator GAMBIT with the objective of good wall function performance.

RESULTS AND DISCUSSION

In order to provide a direct comparison with the available experimental data, results are presented by showing pressure recovery factor values at several axial stations because this factor represents diffuser performance. In addition, to study the physics of flow we insert pressure contours and velocity vectors. The flow computations required about 103 iterations to converge. At the end of every computational run, flow residual are reduced by more than seven orders of magnitude. A sample of residual history is shown in Fig.(4). Results compared with available published experimental data. Fig.(5) presents the variation of pressure recovery through a diffuser for three values of Reynolds number at entrance and compared with these from experimental data. It shows that the pressure recovery increases with the increase in Reynolds number. A good agreement with experimental work, only at =300 where occurred maximum deviation about 25% due to began sharp

change in flow direction at this station. The effect of curvature angle on the performance of diffuser was presented in Fig.(6) which shows that pressure recovery decrease as curvature angle increases, because of increasing the energy losses due to the increase of length of diffuser and existing a secondary flow, also this appear in pressure contours and velocity vector in Figs.(9,10). The pressure recovery behavior with variation of area ratio is shown in Fig (7). Area ratio increase leads to enhance in diffuser performance due to the increase in area, but this enhancement will be limited after AR=2.5 (this is very clear in Fig.(7)), due to increase in intensity of separation, also the effect of increasing in area ratio is clear in Figs.(11,12), which represents pressure contours and velocity vector respectively. The effect of adding a tail channel with constant area at the exit of diffuser on pressure recovery is revealed in Fig.(8). The pressure recovery is increased with the increase of length of tail channel due to increase of the uniformity of flow at the exit of diffuser; this will lead to increase in total pressure

recovery and decrease in velocity as shown in Figs.(13,14).

CONCLUSIONS

It is very important to have a precise simulation tool for prediction turbulent flow through diffusers. So that, Fluent capability to predict the behavior of turbulent, subsonic, and incompressible flow through a 2-D curved diffuser has been implemented. The computations show that the Fluent code gives good result when looking for pressure distribution. Comparison of the pressure recovery factor with the available experimental data summarizes this conclusion.

REFERENCES

[1]T. D. Bello, V. Deppold, and N. J. Georgiadis "Computational Study of Separating Flow in a Planar Subsonic Diffuser" NASA/TM- 2005-213894.

[2]W. L. Zhang, D. D. Knight, and D. Smith "Automated Design of a Three-Dimensional Subsonic Diffuser" J. Propulsion and Power, Vol. 16, No. 6, November-December 2000.

[3]H. Sprenger, "Experimental investigation of straight and curved

diffusers" Mitt. Inst. Aerodyne. Zurich (27)88pp., May 1962.

[4] B. Majumdar and B. Agrawal "Flow Characteristics in Large Area Ratio Curved Diffuser" J. Aerospace engineering 210(G1):55-75, 1996

[5] S. N. Singh, D. P. Agrawal, R. Mohan, and B. Majumdar "Experimental Study of Flow High Aspect Ratio 900 Curved Diffuser" J. Fluid Engineering Vol. 120 pp. 83-89, 1998

[6] Y. D. Choi, H. Lacovides, and B. E. Launder "Numerical Computation of Turbulent Flow in a Square Section 180^0 Bend" J. Fluid Engineering Vol.111 pp.59-67 March 1989.

[7]S. Chang, M. Humphrey, J. A. C, and Modavi "Turbulent Flow through 180^0 Bend" Karlsruhe pp.620-625, 1983.

[8]Al-Annaz, Ammar H. S. "Experimental study on the Performance of Two-Dimensional Curved Diffuser" MSc. Thesis, University of Tikrit 2003.

[9] Fluent 6.3 Documents, Fluent Inc. 2006 from the help of program in the CD of Fluent.

[10] P. Spalart and S. Allmaras. A one-equation turbulence model for aerodynamic flows. Technical Report AIAA-92-0439, American Institute of Aeronautics and Astronautics, 1992.

Table (1) model constants[10]

Const	Cb1	Cb2	†~	Cv1	Cw1	Cw2	Cw3	
Value	0.1355	0.622	2/3	7.1	$\dfrac{C_{b1}}{\mid^2} < \dfrac{\theta_1 < C_{b2}:}{\dagger\sim}$	0.3	2.0	0.4187

Table(2) Details of cases study

Cases Variables	Comparison case study	Effect of curvature angle	Effect of area ratio	Effect of adding tail channel
	90^0	$30^0, 60^0, 90^0$	90^0	90^0
AR	2.5	2.5	2, 2.5, 3	2.5
L/D	0	0	0	0,1, 2
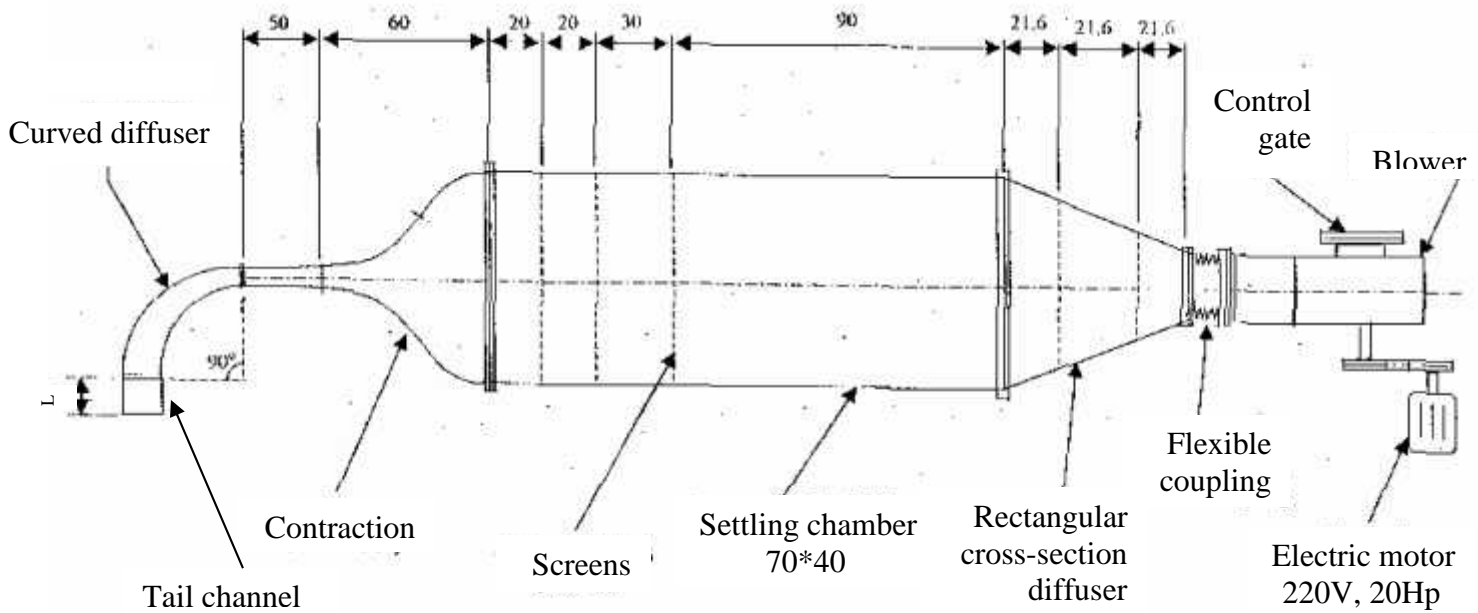
Fig.(1) Detailed Schematic of Diffuser Layout[6]   All dimensions in (cm)

Outflow
B.C.

No-slip wall
B.C.

Velocity
inlet B.C.
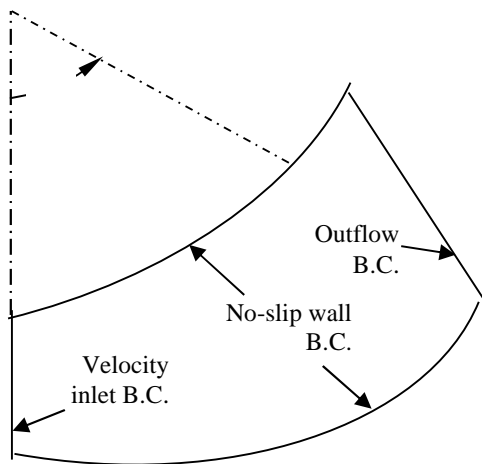
**Fig.(2) Outline of computational domain
with boundary conditions**
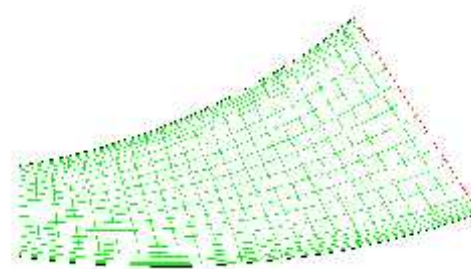
**Fig.(3) Close-up of Grid Generation
(Two-dimensional, structured, Quad.
Mesh) for ($\theta=30^0$)**
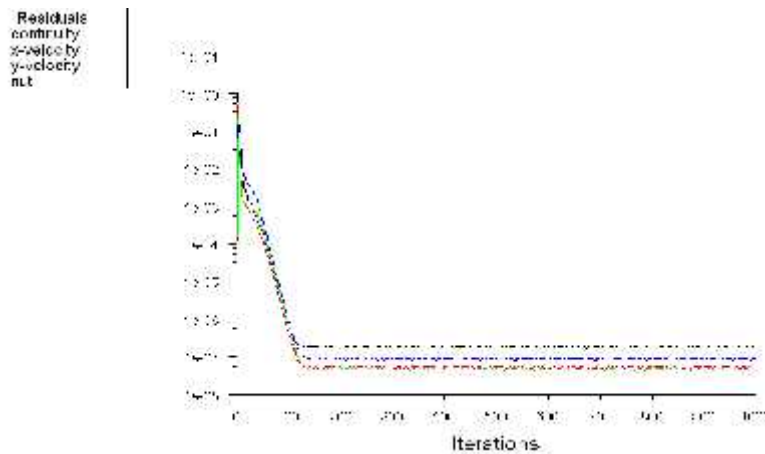
Fig.4 Residual History of Solution Convergence
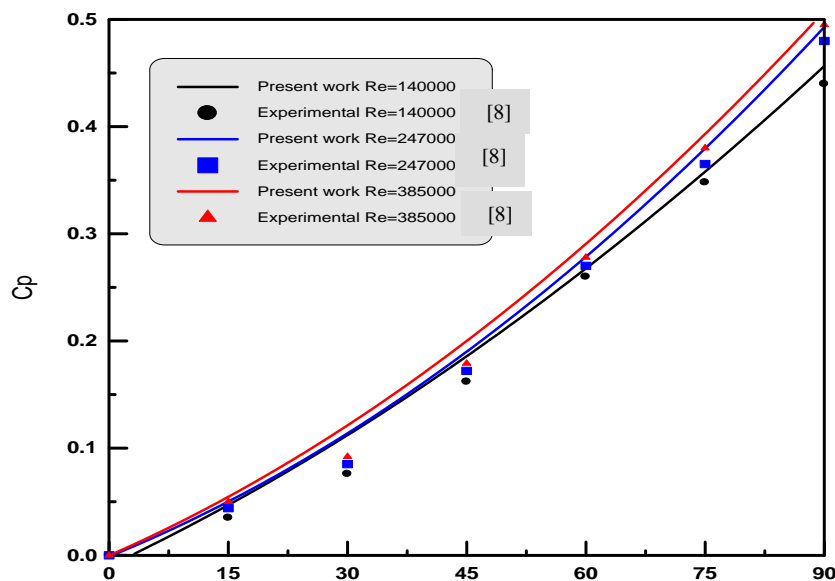
Fig.5 Pressure Recovery Distribution along Diffuser for Different Entrance Reynolds No.
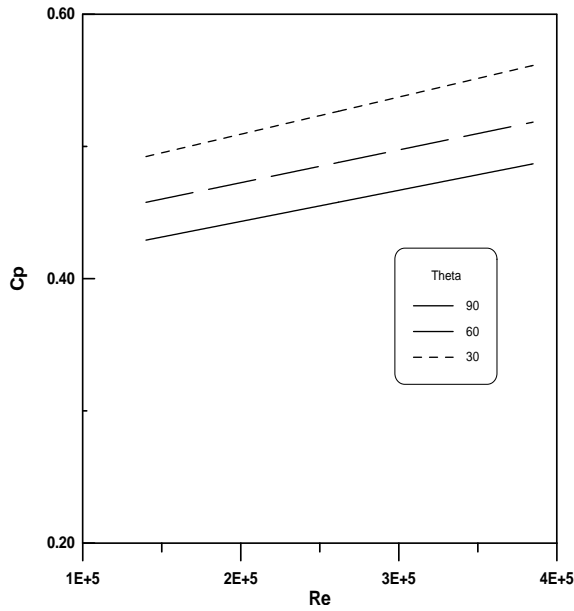
Fig.6 Variation of Pressure Recovery Factor via Re No. for Different Curvature Angle (AR=2.5, L/D=0)
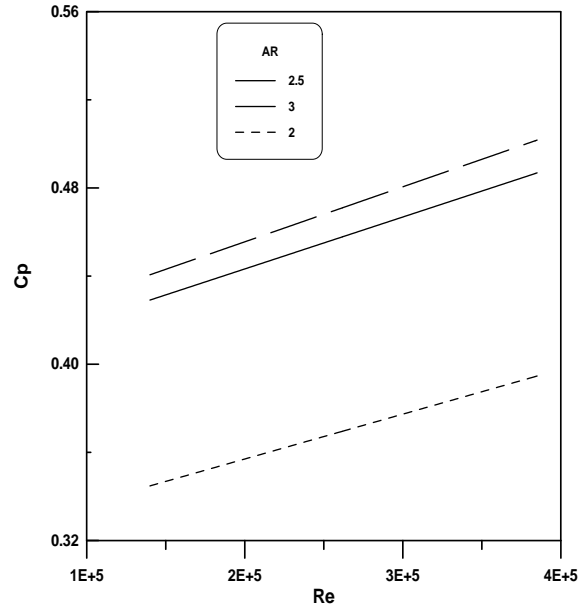
Fig.7 Variation of Pressure Recovery Factor via Re No. for Different Area Ratio (=90⁰,L/D=0)
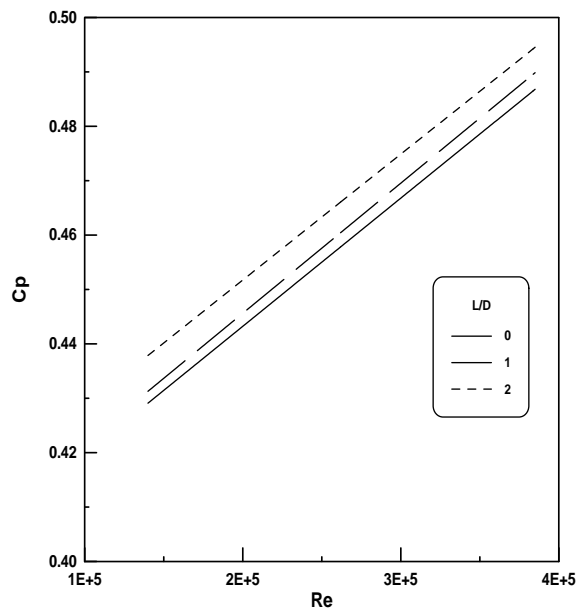
Fig.8 Variation of Pressure Recovery Factor via Re No. for Different Tail Channel Length (=90⁰,AR=2.5)

a- θ=30⁰

a- θ=30⁰

b- θ=60⁰

b- θ=60⁰

c- θ=90⁰

c- θ=90⁰
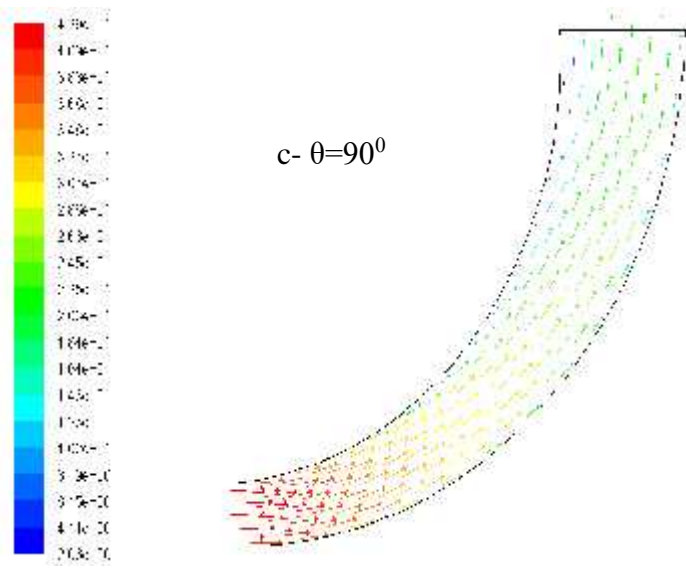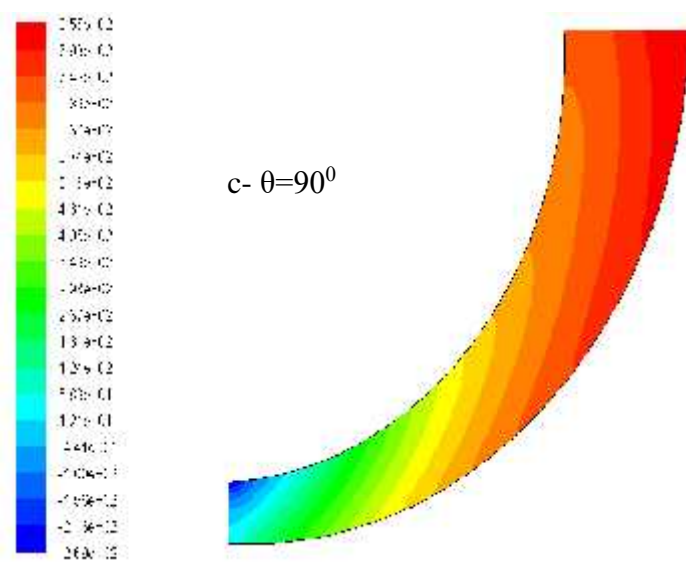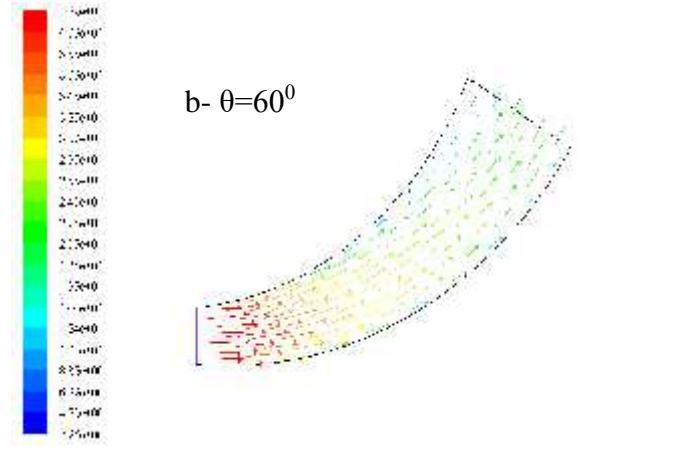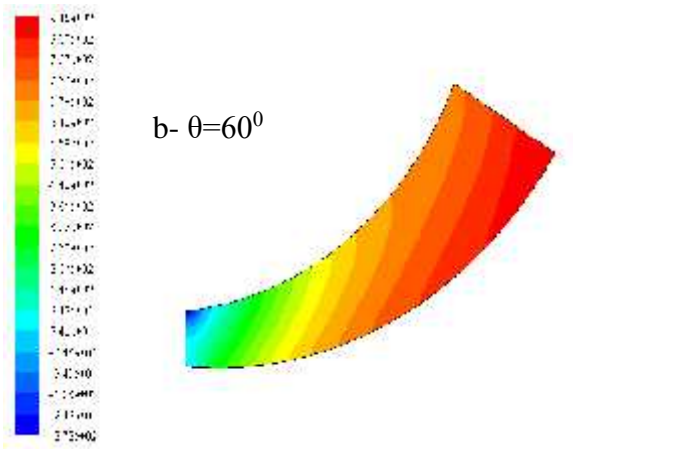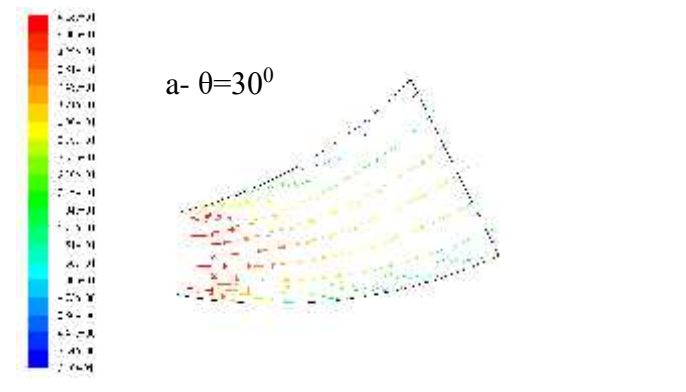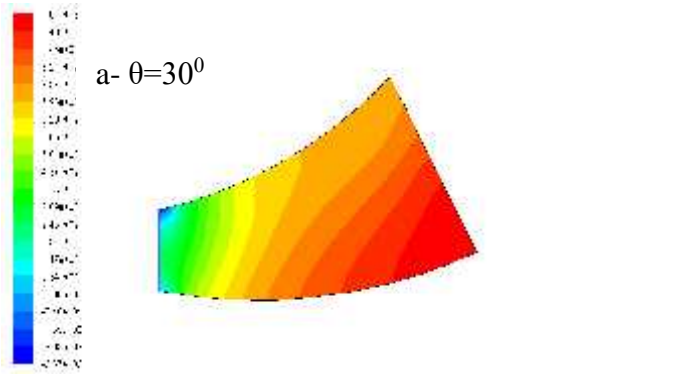
**Fig.9 Static Pressure Contours
for Different Curvature Angle
(AR=2.5, L/D=0)**

**Fig.10 Velocity Vector Magnitude
for Different Curvature Angle
(AR=2.5, L/D=0)**

a- AR=2

a- AR=2

b- AR=2.5

b- AR=2.5

c- AR=3

c- AR=3
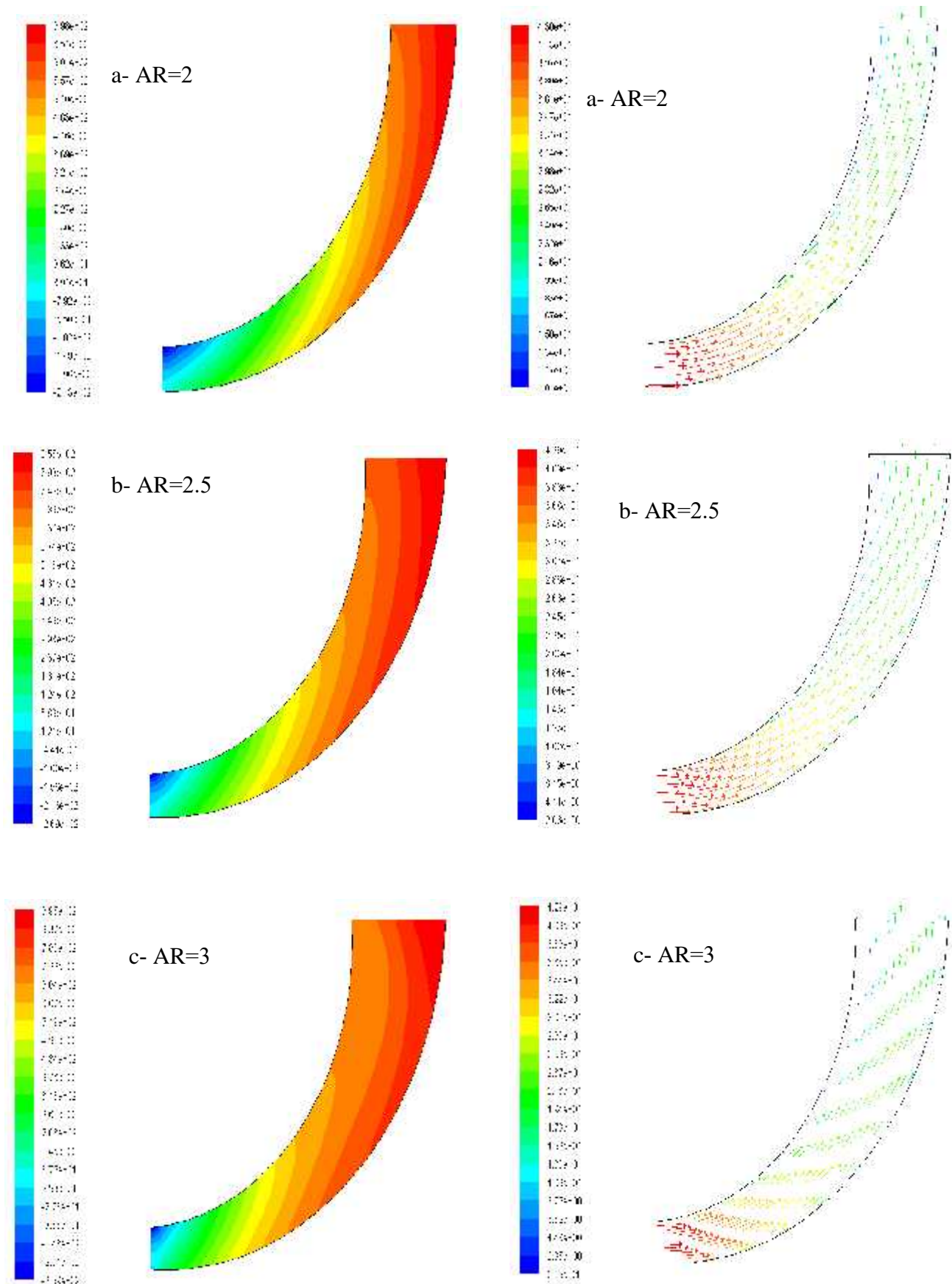
**Fig.11 Static Pressure Contours
for Different Area Ratio(θ=90^0,**

**Fig.12 Velocity Vector Magnitude for
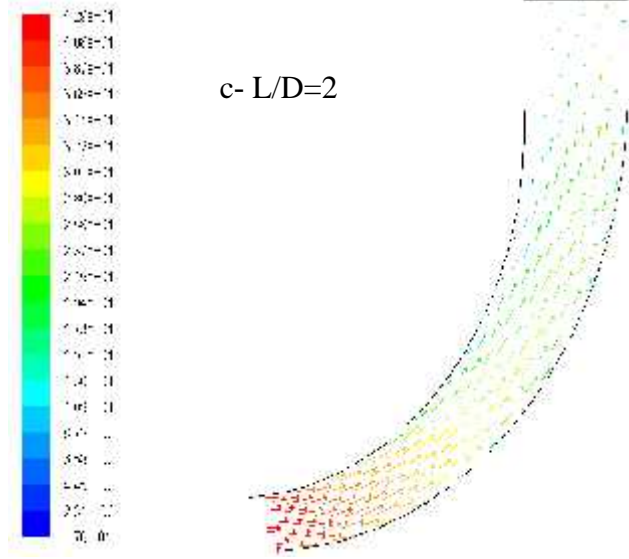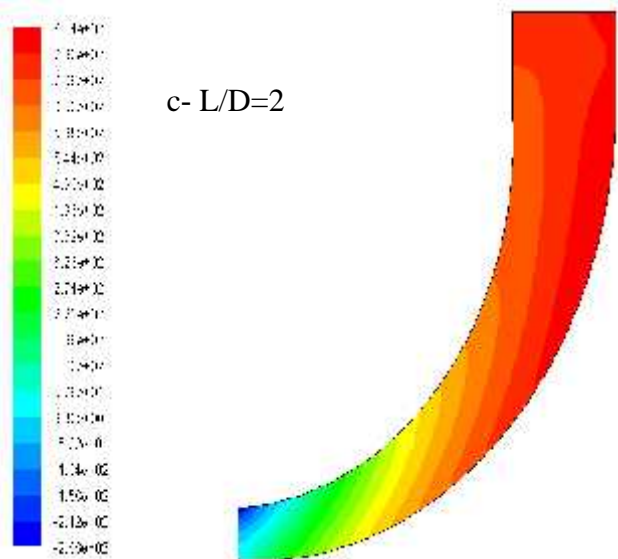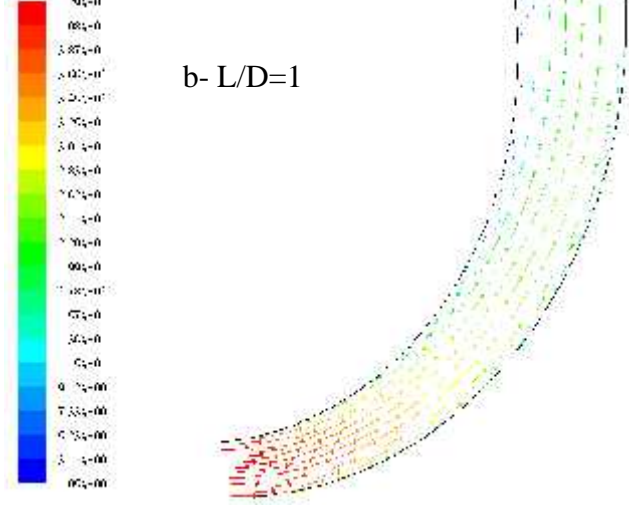Different Area Ratio(θ=90^0, L/D=0)**

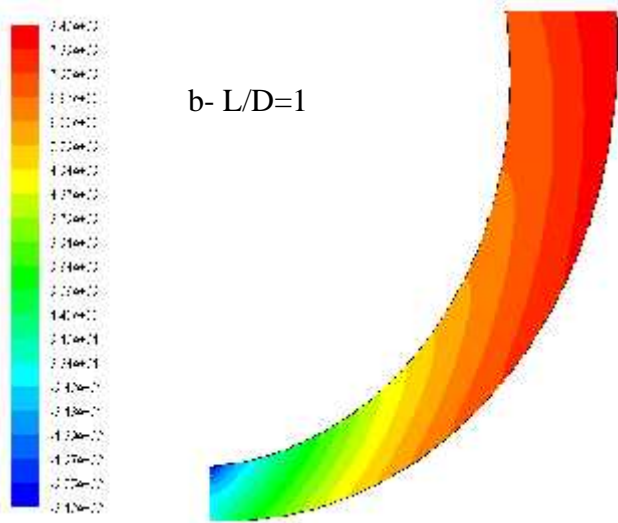a- L/D=0

b- L/D=1

c- L/D=2
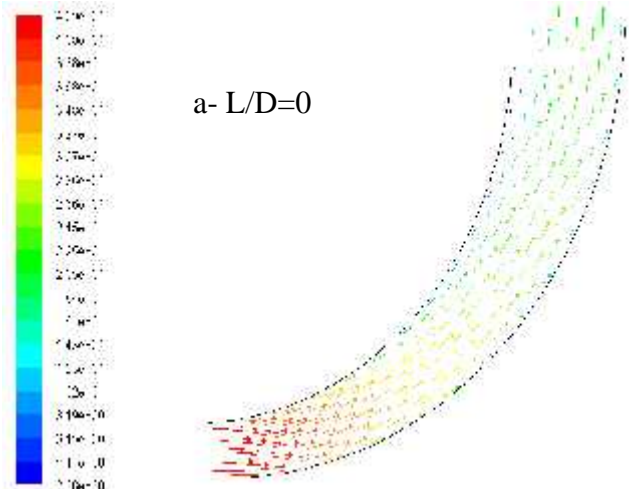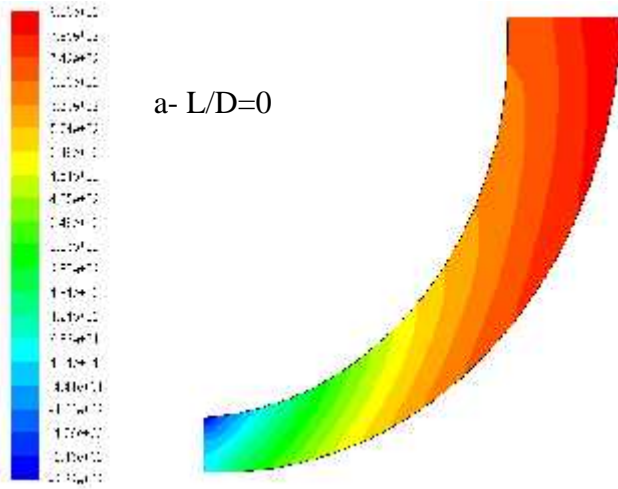
Fig.13 Static Pressure Contours for Different Tail Channel Length(θ=90⁰,

a- L/D=0

b- L/D=1

c- L/D=2

Fig.14 Velocity Vector Magnitude for Different Tail Channel Length(θ=90⁰, AR=2.5)

تحقق عددي لأداء ناشرة ثنائية البعد مقوسة

خلف إبراهيم حمادة

مدرس مساعد

سم الهندسة الميكانيكية- جامعة تكريت

الخلاصة

تناول البحث الحالي استقصاء عددي لميزة الجريان اللزج دون الصوتي خلال ناشرة مقوسة باستخدام احد الرمجيات التجارية المستخدمة في حل مسائل حسابات حركة الموائع. فرض الجريان خلال الناشرة ثنائي البعد، مضطرب، غير انضغاطي وتام النمو. أُستخدم البرنامج Fluent6.3 في الحل العددي لمسألة البحث باعتماد نموذج Spalart-Allmaras لتمثيل خواص الاضطراب في الجريان. تم بناء النماذج والتوليد الشبكي الخاص بها بواسطة برنامج GAMBIT، حيث تم اعتماد نموذج ثنائي البعد راعي الأضلاع. تم مقارنة نتائج الحالة الدراسية (AR=2.5, 90^0=) مع النتائج العملية المتاحة وكان هناك توافق جيد. حيث دُرس تأثير كل من زاوية التقوس ونسبة مساحة المخرج إلى المدخل وإضافة قناة ثابتة المقطع في النهاية على أداء الناشرة وخواص الجريان خلالها وتم عرض النتائج على شكل مخططات كنتورية للضغط ومتجهات للسرعة ومنحنيات معامل استرجاع الضغط لجميع الحالات المذكورة أعلاه.

الكلمات الدالة: أداء ناشرة مقوسة، ديناميك موائع حسابي، جريان اضطرابي.